The Astronomical Journal, 149:5 (12pp), 2015 January doi:10.1088/0004-6256/149/1/5

THE SOLAR NEIGHBORHOOD. XXXV. DISTANCES TO 1404 M DWARF SYSTEMS WITHIN 25 PC IN THE SOUTHERN SKY

Jennifer G. Winters[1,8], Todd J. Henry[2,8], John C. Lurie[3,8], Nigel C. Hambly[4], Wei-Chun Jao[1,8], Jennifer L. Bartlett[5,8], Mark R. Boyd[2,8], Sergio B. Dieterich[1,8], Charlie T. Finch[5,8], Altonio D. Hosey[2,8], Philip A. Ianna[2,8], Adric R. Riedel[6,8], Kenneth J. Slatten[2], and John P. Subasavage[7,8]

[1] Department of Physics and Astronomy, Georgia State University, Atlanta, GA 30302-4106, USA; winters@astro.gsu.edu; thenry@astro.gsu.edu; jao@astro.gsu.edu; boyd@astro.gsu.edu; dieterich@astro.gsu.edu; hosey@astro.gsu.edu
[2] RECONS Institute, Chambersburg, PA 17201, USA; kslatten@cpinternet.com; philianna3@gmail.com
[3] Astronomy Department, University of Washington, Seattle, WA 98195, USA; lurie@uw.edu
[4] Scottish Universities Physics Alliance (SUPA), Institute of Astronomy, University of Edinburgh, Royal Observatory, Blackford Hill, Edinburgh EH9 3HJ, Scotland, UK; nch@roe.ac.uk
[5] US Naval Observatory, 3450 Massachussetts Ave. NW, Washington, DC 20392, USA; finch@usno.navy.mil; jennifer.bartlett@usno.navy.mil
[6] Hunter College/American Museum of Natural History, NYC, NY, USA; ar494@hunter.cuny.edu
[7] US Naval Observatory, Flagstaff Station, 10391 West Observatory Road, Flagstaff, AZ 86001, USA; jsubasavage@nofs.navy.mil
Received 2014 June 27; accepted 2014 July 25; published 2014 December 1

ABSTRACT

We present trigonometric, photometric, and photographic distances to 1748 southern ($\delta \leqslant 0°$) M dwarf systems with $\mu \geqslant 0\farcs18\ \mathrm{yr}^{-1}$, of which 1404 are believed to lie within 25 pc of the Sun. The stars have $6.67 \leqslant V_J \leqslant 21.38$ and $3.50 \leqslant (V_J - K_s) \leqslant 9.27$, covering the entire M dwarf spectral sequence from M0.0 V through M9.5 V. This sample therefore provides a comprehensive snapshot of our current knowledge of the southern sky for the nearest M dwarfs that dominate the stellar population of the Galaxy. Roughly one-third of the 1748 systems, each of which has an M dwarf primary, have published high quality parallaxes, including 179 from the REsearch Consortium On Nearby Stars astrometry program. For the remaining systems, we offer photometric distance estimates that have well-calibrated errors. The bulk of these (~700) are based on new $V_J R_{KC} I_{KC}$ photometry acquired at the CTIO/SMARTS 0.9 m telescope, while the remaining 500 primaries have photographic plate distance estimates calculated using SuperCOSMOS $B_J R_{59F} I_{IVN}$ photometry. Confirmed and candidate subdwarfs in the sample have been identified, and a census of companions is included.

Key words: parallaxes – solar neighborhood – stars: distances – stars: low-mass – stars: statistics – techniques: photometric

Supporting material: machine-readable and VO tables

1. INTRODUCTION

There is great interest in developing a comprehensive list of nearby M dwarfs for studies of the Milky Way's stellar population, both as astrophysically compelling individual objects and as prime targets for exoplanet and SETI search lists. These stars, typically called red dwarfs, dominate the stellar population of our Galaxy, accounting for more than 75% of all main sequence stars in the solar neighborhood (Henry et al. 2006).[9] Yet, distance determinations for red dwarfs have remained a challenge. Trigonometric parallaxes are the optimal tool for calculating distances, but because of observing time and resource constraints, distance estimation methods are attractive alternatives and are often a preliminary step in determining which targets are to be added to parallax programs.

There are two primary sources of trigonometric parallax data currently available. *The General Catalogue of Trigonometric Stellar Parallaxes, Fourth Edition* (van Altena et al. 1995), often called the Yale Parallax Catalog (hereafter YPC), is a valuable compendium of ground-based parallaxes published prior to 1995 and includes about half of the southern M dwarf parallaxes measured to date. The *Hipparcos* mission (initial release by Perryman et al. 1997, and the updated results by van Leeuwen 2007; hereafter HIP) updated many of those parallaxes, and contributed almost two hundred new measurements for mostly bright ($V \lesssim 12.5$) southern M dwarfs.

Since then, the REsearch Consortium On Nearby Stars (RECONS) group has measured a substantial number of parallaxes to nearby stars to date, adding 154 M dwarf systems to the 25 pc census (Jao et al. 2005, 2014; Costa et al. 2005; Henry et al. 2006; Costa et al. 2006; Subasavage et al. 2009; Riedel et al. 2010; Jao et al. 2011; Riedel et al. 2011; von Braun et al. 2011; Mamajek et al. 2013; Dieterich et al. 2014; Riedel et al. 2014), published in *The Solar Neighborhood* series of papers (hereafter TSN) in *The Astronomical Journal*. This effort has increased the number of M dwarf systems with accurate trigonometric parallaxes in the southern sky by 35%, with several hundred more determinations underway.

Both in addition to and in combination with proper motion surveys, optical photometry has historically been used to identify and characterize nearby stars. The first generation of sky surveys for intrinsically faint, nearby stars included the work of Luyten (1979a, 1979b, 1980a, 1980b) and Giclas et al. (1971, 1978). The work continued into the late twentieth century via the efforts of Bessel (1990); Bessell (1991), Weis (1984, 1986, 1987, 1988, 1991a, 1991b, 1993, 1994, 1996, 1999), Wroblewski & Torres (1989, 1990, 1991, 1992, 1994, 1995, 1996, 1997, 1998), and Wroblewski & Costa (1999, 2000, 2001). More recent surveys include the SAAO group

[8] Visiting Astronomer, Cerro Tololo Inter-American Observatory. CTIO is operated by AURA, Inc. under contract to the National Science Foundation.
[9] Updated counts provided at www.recons.org

(Kilkenny & Cousins 1995; Kilkenny et al. 1998, 2007; Koen et al. 2002, 2010; Reid et al. 2001, 2002, 2003, 2004), Lépine (Lépine et al. 2002, 2003; Lépine 2005a, 2005b, 2008; Lépine & Gaidos 2011), the USNO (Finch et al. 2010, 2012), and Deacon (Deacon et al. 2005a, 2005b; Deacon & Hambly 2007; Deacon et al. 2009a, 2009b), as well as RECONS' efforts in the southern sky (Hambly et al. 2004; Henry et al. 2004; Subasavage et al. 2005a, 2005b; Finch et al. 2007; Winters et al. 2011; Boyd et al. 2011a, 2011b). This work is a continuation in that tradition, and includes a comprehensive assessment of the known population of red dwarfs in the southern sky, with a particular emphasis on those closer than a 25 pc horizon.

2. DEFINITION OF THE SAMPLE

We have developed a list of 1748 southern ($\delta \leqslant 0°$) stellar systems containing M dwarf primaries.[10] Here we define an M dwarf to be a star with $3.50 \leqslant (V_J - K_s) \leqslant 9.27$, corresponding to spectral types M0.0 V–M9.5 V, where the red cut-off has been defined by Henry et al. (2004). This list is a combination of objects with existing high quality parallaxes, objects for which we have measured photometry as part of our southern astrometry/photometry program, and known objects that were recovered during our SuperCOSMOS-RECONS (SCR) proper motion searches for new nearby stars. To eliminate any red giants that may slip into this sample and to be consistent with the proper motion cut-off of Luyten, we limit our targets to those with proper motions, μ, greater than $0\farcs18\ \mathrm{yr}^{-1}$.

Table 1 provides the observed data for the entire sample, including the name of the M dwarf primary, the number of known components in the system, coordinates (J2000.0), proper motion magnitude and position angle with reference, the weighted mean of the published trigonometric parallaxes and the error, the number of parallaxes included in the weighted mean and references, SuperCOSMOS $B_J R_{59F} I_{IVN}$ plate magnitudes (hereafter simply *BRI*), $V_J R_{KC} I_{KC}$ (hereafter simply *VRI*) measured by RECONS at Cerro Tololo Inter-American Observatory (CTIO) and the number of observations, or *VRI* from a trusted source and the reference, and 2MASS JHK_s magnitudes. The table is divided into the 1404 systems within 25 pc (top) and the 344 systems beyond 25 pc (bottom). A number in parentheses next to the number of components column indicates how many of the components are included in the photometry. All proper motions are from SuperCOSMOS, except where noted.[11] "*J*" next to a magnitude indicates that light from a close companion has resulted in blended photometry. A "u" next to the photometry reference code indicates that we have previously published photometry for this object, but have since then acquired more data and updated the value.

Each system has at least one of three different distance determinations, listed in Table 2, with the best distance either photographic (*pltdist*, 500 systems), photometric (*ccddist*, 667), or trigonometric (*trgdist*, 581).[12] Most of the systems presented here have more than one type of distance measurement. For example, a system with a trigonometric parallax published by our group is likely to also have a *ccddist* and a *pltdist* because we first estimated a distance photometrically from SuperCOSMOS plates, then measured *VRI* photometry to yield a more accurate *ccddist*, then observed the system for a parallax measurement, which provides *trgdist*. We rank the quality of the distances by the errors associated with each method: *pltdists* from photographic photometry rank third (errors at least 26%), *ccddists* from *VRI* photometry rank second (errors at least 15%), and *trgdists* derived from accurate trigonometric parallaxes are the best available (errors $< 5\%$). Figure 1 illustrates the distribution of all 1748 systems on the sky.

2.1. Multiples

We are currently involved in an all-sky study of the multiplicity of M dwarfs using a sample of ~1300 red dwarfs having accurate trigonometric parallaxes placing them within 25 pc. This project involves three search methods to identify and confirm companions at separations from $0\farcs1$ to $600''$: a robotic adaptive optics search (0.1–$2''$), an *I*-band imaging search (~1–$10''$), and a common proper motion search (~5–$600''$). Because most of these results will be published in a future paper, we give only the number of known components in each system in Table 1. An exhaustive literature search was not performed. Based on this cursory search, the number of known multiples in the 25 pc portion of the sample is 164, which results in a multiplicity fraction of 12%. This is one-half to one-third the value that is expected (Henry 1991; Fischer & Marcy 1992; Janson et al. 2012, 2014), so it is clear that more work is needed to determine the true multiplicity fraction of even the nearest M dwarfs. Of the 164 multiples, 114 have *pltdists* that are based on unresolved photometry. These are typically multiples with magnitude differences at $BRI \lesssim 2$ and with separations $<4''$. Of these 114 with *pltdists*, 96 systems have *ccddists* based on unresolved photometry because their separations are $<1''$. In addition, photometry from the SAAO extracted from the literature (references in Section 1) uses apertures 21–$31''$ in diameter, so additional components have likely been included in the photometric values used to derive *ccddists*. The comprehensive survey of red dwarf multiplicity mentioned above constitutes a major fraction of the first author's PhD work, so a much more careful treatment of red dwarf multiples within 25 pc is forthcoming. For now, we note that the reader should be cautious when applying the *pltdist* or *ccddist* values given in Table 2 for multiple systems.

3. DATA

3.1. $B_J R_{59F} I_{IVN}$ Plate Photometry

Plate magnitudes from SuperCOSMOS are given in Table 1 for all but a few systems and are rounded to the nearest

[10] We refer to any collection of stars and their companion brown dwarfs and/or exoplanets as a system, including single M dwarfs not currently known to have any companions. Systems that contain a white dwarf component have been omitted, as the white dwarf was initially the brighter primary component.

[11] Some of the proper motion values from the SuperCOSMOS Sky Survey for SCR objects presented here differ slightly from those in the original discovery papers. For the new values, a more comprehensive method has been used that provides multiple measurements of proper motion between various plate pairs, while before only a single value was available that incorporated all plates into the solution simultaneously. The proper motions provided here are those that yield consistent values among multiple determinations and are preferred.

[12] The term *pltdist* is used for the remainder of the paper to indicate a distance estimate that combines SuperCOSMOS plate *BRI* and 2MASS JHK_s magnitudes, as discussed in Section 4.1. The plate R_{59F} magnitude is the second, more recent *R* epoch measurement of the two available in the SuperCOSMOS Sky Survey. The term *ccddist* is used to indicate a distance estimate that combines CCD *VRI* and 2MASS JHK_s magnitudes, as discussed in Section 4.2. The term *trgdist* is used for those objects for which an accurate trigonometric parallax has been measured, as discussed in Section 3.4.

Table 1
Observed Data for Southern Red Dwarf Systems

Name	# Comp.	R.A.	Decl.	μ ($''$yr^{-1})	P.A. (deg)	Ref	π (mas)	π error (mas)	# π	Ref	B_J (mag)	R_{59F} (mag)	I_{IVN} (mag)	V_J (mag)	R_{KC} (mag)	I_{KC} (mag)	# Nts/Ref	J (mag)	H (mag)	K_s (mag)
(1)	(2)	(3)	(4)	(5)	(6)	(7)	(8)	(9)	(10)	(11)	(12)	(13)	(14)	(15)	(16)	(17)	(18)	(19)	(20)	(21)
2MA0000-1245	1	00 00 28.7	−12 45 16	0.191	228.6	41	...	...	...	...	...	19.26	15.88	20.78	18.71	16.27	1/	13.20	12.45	11.97
LTT09844	1	00 00 46.9	−35 10 06	0.403	106.3	1	...	...	...	...	13.48	11.30	10.21	...	...	...	...	9.12	8.48	8.28
GJ1001	3(1)	00 04 36.5	−40 44 03	1.636	159.7	1	79.87	3.75	2	25,63	14.21	11.83	10.06	12.83	11.62	10.08	4/25u	8.60	8.04	7.74
G158-025	1	00 04 40.3	−09 52 42	0.267	170.6	1	...	...	...	...	14.47	12.52	10.92	...	...	...	...	9.77	9.10	8.82
SIP000–2058	1	00 04 41.5	−20 58 30	0.826	090.6	1	...	...	...	...	21.86	18.85	15.65	19.94	17.81	15.36	2/	12.40	11.83	11.40
GJ0001	1	00 05 24.4	−37 21 27	6.106	112.5	28	230.32	0.90	2	63,64	10.10	7.91	6.28	8.54	7.57	6.41	/5	5.33	4.83[c]	4.52
LP644-034	1	00 05 34.9	−06 07 07	0.218	111.7	1	...	...	...	...	13.85	11.75	9.92	...	...	...	...	9.26	8.65	8.41
LP644-039	1	00 06 13.1	−02 32 11	0.305	101.3	1	...	...	...	...	15.38	13.34	10.91	14.62	13.42	11.84	/45	10.22	9.60	9.30
LHS1019	1	00 06 19.2	−65 50 26	0.564	158.7	1	59.85	2.64	1	64	13.13	10.92	8.98	12.17	11.11	9.78	/34	8.48	7.84	7.63
GJ1002	1	00 06 43.2	−07 32 17	2.041	204.0	63	213.00	3.60	1	63	15.04	12.34	9.88	13.84	12.21	10.21	3/	8.32	7.79	7.44

Notes. A "J" next to a photometry value indicates that the magnitude is blended due to a close companion.
A "u" next to the photometry reference code indicates an updated value since the last publication from the RECONS group due to aquisition of more data.

References. (1) This paper, (2) Andrei et al. (2011), (3) Anglada-Escudé et al. (2012), (3) Benedict et al. (2002), (5) Bessel (1990), (6) Bessell (1991), (7) Biller & Close (2007), (8) Boyd et al. (2011a), (9) Costa and Méndez (2003), (10) Costa et al. (2005), (11) Costa et al. (2006), (12) Deacon & Hambly (2001), (13) Deacon et al. (2005a), (14) Deacon et al. (2005b), (15) Deacon & Hambly (2007), (16) Dieterich et al. (2014), (17) Dupuy & Liu (2012), (18) Fabricius & Makarov (2000), (19) Faherty et al. (2012), (20) Finch et al. (2010), (21) Finch et al. (2012), (22) Gatewood et al. (2003), (23) Gizis et al. (2011), (24) Henry et al. (2004), (25) Henry et al. (2006), (26) Henry et al. (1997), (27) Hershey & Taff (1998), (28) Høg et al. (2000), (29) Jao et al. (2005), (30) Jao et al. (2011), (31) Jao et al. (2014), (32) Kilkenny et al. (2007), (33) Koen et al. (2002), (34) Koen et al. (2010), (35) Lépine (2008), (36) Luyten (1979a), (37) Luyten (1980a), (38) Luyten (1980b), (39) Monet et al. (2003), (40) Patterson et al. (1998), (41) Phan-Bao (2011), (42) Pokorny et al. (2003), (43) Pokorny et al. (2004), (44) Reid et al. (2002), (45) Reid et al. (2003), (46) Reid et al. (2004), (47) Riedel et al. (2010), (48) Riedel et al. (2011), (49) Riedel et al. (2014), (50) Ruiz et al. (2001), (51) Ruiz et al. (1993), (52) Schilbach et al. (2009), (53) Schmidt et al. (2007), (54) Scholz et al. (2004), (55) Shkolnik et al. (2012), (56) Smart et al. (2007), (57) Smart et al. (2010), (58) Söderhjelm (1999), (59) Subasavage et al. (2005a), (60) Subasavage et al. (2005b), (61) Tinney et al. (1995), (62) Tinney (1996), (63) van Altena et al. (1995), (64) van Leeuwen (2007), (65) von Braun et al. (2011), (66) Weis (1991a), (67) Weis (1991b), (68) Weis (1993), (69) Weis (1996), (70) Weis (1999), (71) Winters et al. (2011), (72) Wolf & Reinmuth (1925), (73) Wroblewski & Torres (1994), (74) Wroblewski & Torres (1997).

[a] The weighted mean parallax includes the parallax of both the primary and the secondary components.
[b] The HIP parallax is markedly different from that published in YPC and has an error of ~45 mas.
[c] 2MASS magnitude error greater than 0.05 mag.

(This table is available in its entirety in machine-readable and Virtual Observatory (VO) forms.)

Table 2
Derived Data for Southern Red Dwarf Systems

Name	R.A.	Decl.	d_{plt} (pc)	σ_{tot} (pc)	# Rel	d_{ccd} (pc)	σ_{tot} (pc)	# Rel	d_{trig} (pc)	σ_{trig} (pc)	# π	d_{best} (pc)	d type
(1)	(2)	(3)	(4)	(5)	(6)	(7)	(8)	(9)	(10)	(11)	(12)	(13)	(14)
2MA0000-1245	00 00 28.7	−12 45 16	22.2	7.6	7	23.1	4.0	11	...	...	...	23.1	ccd
LTT09844	00 00 46.9	−35 10 06	23.5	7.4	11	...	...	...	...	...	...	23.5	plt
GJ1001	00 04 36.5	−40 44 03	11.2	3.4	11	12.5	1.9	12	12.5	0.6	2	12.5	trg
G158-025	00 04 40.3	−09 52 42	24.5	7.4	11	...	...	...	...	...	...	24.5	plt
SIP0004-2058	00 04 41.5	−20 58 30	14.9	6.8	10	18.6	3.0	11	...	...	...	18.6	ccd
GJ0001	00 05 24.4	−37 21 27	3.7	1.0	11	5.6	0.9	11	4.3	0.0	2	4.3	trg
LP644-034	00 05 34.9	−06 07 07	23.0	6.2	11	...	...	...	...	...	...	23.0	plt
LP644-039	00 06 13.1	−02 32 11	27.3	9.2	11	21.9	3.9	12	...	...	...	21.9	ccd
LHS1019	00 06 19.2	−65 50 26	16.1	4.6	11	16.6	2.6	12	16.7	0.7	1	16.7	trg
GJ1002	00 06 43.2	−07 32 17	6.8	2.1	11	5.4	1.0	12	4.7	0.1	1	4.7	trg

Notes.
[a] The weighted mean distance includes that of both the primary and the secondary components.
(This table is available in its entirety in machine-readable and Virtual Observatory (VO) forms.)

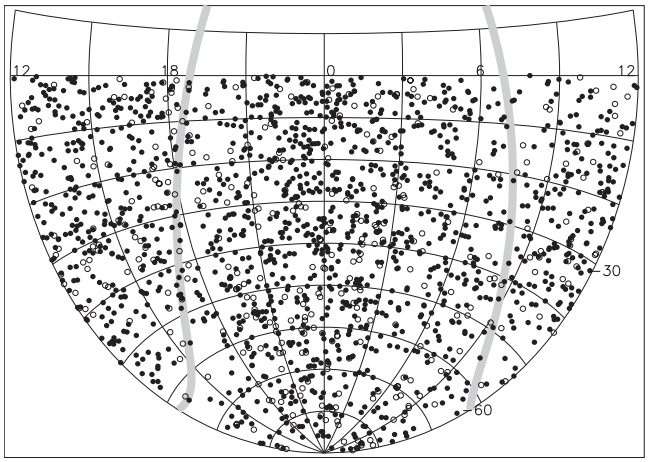

Figure 1. Distribution of the entire sample of 1748 M dwarf systems on the southern sky in R.A. and Decl.. Solid points indicate the 1404 systems within 25 pc, while open points indicate the 344 systems beyond 25 pc. The Galactic plane has been plotted in gray.

hundredth magnitude.[13] Errors are typically 0.3 mag for magnitudes fainter than 15, with larger errors for brighter objects due to systematic errors (Hambly et al. 2001). Derived *pltdists* in Table 2 for SCR discoveries have been previously presented in the TSN papers, but we provide 1457 new *pltdists* here for previously known objects. Additional SuperCOSMOS queries were recently done in an effort to provide as many *pltdists* as possible. Due to an improved SuperCOSMOS photometric calibration,[14] some magnitudes will be slightly different from those reported in previous papers in this series; the values presented here are preferred. In some cases, a match was not found because very red objects were not always recovered from the *B* plate, because of very high proper motion, or because of source mergers or corruption. All matches were visually confirmed and were doublechecked using the SuperCOSMOS proper motions and *BRI* magnitudes.

3.2. $V_J R_{KC} I_{KC}$ CCD Photometry

We have measured *VRI* photometry for 799 of the systems presented here as a part of our astrometry/photometry program, primarily at the CTIO/SMARTS 0.9 m, with a few measurements from the CTIO/SMARTS 1.0 m (see Jao et al. 2005; Henry et al. 2006 for details on the astrometry; see Winters et al. 2011 for details on the photometry). The observations were made between 1999 and 2013. The photometry was typically acquired for these nearby star candidates based upon *pltdists* from our SuperCOSMOS trawls or from other proper motion or photometric surveys such as those listed in Section 1.

All of our *VRI* data, given in Table 1, were reduced using IRAF and are on the Johnson–Kron–Cousins system.[15] Calibration frames taken at the beginnings of nights were used for typical bias subtraction and dome flat-fielding. Standard star fields from Graham (1982), Bessel (1990), and/or Landolt (1992, 2007, 2013) were observed multiple times each night in order to derive transformation Equations and extinction curves. In order to match those used by Landolt, apertures 14″ in diameter were used to determine the stellar fluxes, except in cases where close contaminating sources needed to be deblended. In these cases, smaller apertures were used and aperture corrections were applied. As outlined in Winters et al. (2011), photometric errors are typically 30 mmag for the *V*-band and 20 mmag for both the *R*- and *I*-bands. Further details about the data reduction procedures, transformation Equations, etc., can be found in Jao et al. (2005) and Winters et al. (2011).

An additional 369 primaries were found to have high quality optical photometry available from the literature, primarily from Bessell, Weis, and the SAAO group.[16] Among these, 214 already have parallaxes that place them within 25 pc, while an additional 109 have a *ccddist* that place them within 25 pc. The *R* and *I* photometric values from Weis have all been transformed to the Johnson–Kron–Cousins system via the

[13] The wavelength ranges for the B_J, R_{59F}, and I_{IVN} filters are 3950–5400 Å, 5900–6900 Å, and 7150–9000 Å, respectively (Morgan 1995, p. 137).

[14] The recommended access point for the current version of the photometrically calibrated SuperCOSMOS data is the SuperCOSMOS Science Archive, found at http://surveys.roe.ac.uk/ssa. Details of the photometric calibration procedure are available in the online documentation at http://surveys.roe.ac.uk/ssa/dboverview.html#mags.

[15] The central wavelengths for the V_J(old), V_J(new), R_{KC}, and I_{KC} filters are 5438, 5475, 6425, and 8075 Å, respectively. See Jao et al. (2011) for a discussion of the nearly identical V_J(old) and V_J(new) filters.

[16] References given in Table 1.

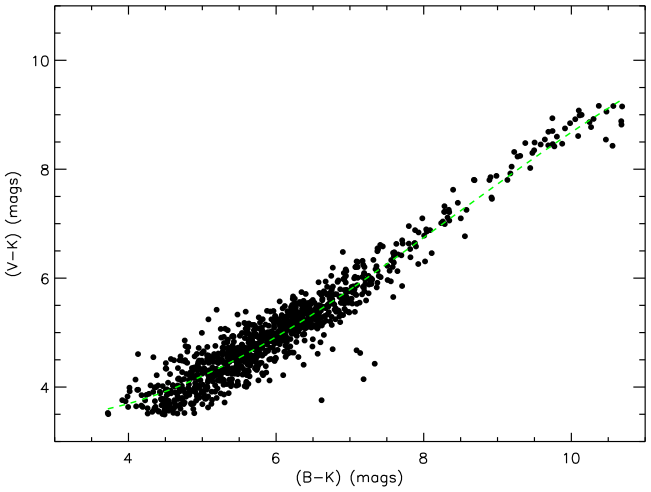

Figure 2. Comparison of the CCD $(V - K)$ color to the plate $(B - K)$ color for more than 1000 objects. Known multiples with blended photometry are not included. The dashed line indicates a third order polynomial fit (given in Section 3.2) that provides an estimated CCD V magnitude, given a measured plate B magnitude for red objects and a known 2MASS K magnitude.

color relations given in Bessell & Weis (1987) so that all *VRI* values in Table 1 are on the same photometric system. SOAR/SOI (SOAR Optical Imager) photometry from Dieterich et al. (2014) has also been converted to the Johnson–Kron–Cousins system using methods described in that paper.

A comparison of $(V_{CCD} - K_s)$ versus $(B_{plt} - K_s)$ for 1026 objects for which both plate B and CCD V photometry is available is shown in Figure 2. Known close binaries for which the photometry is blended have been omitted. A third order polynomial fit,

$$(V_J - K_s) = 4.939 - 1.174*\left(B_{plt} - K_s\right) + 0.256*\left(B_{plt} - K_s\right)^2 - 0.010*\left(B_{plt} - K_s\right)^3$$

permits users of SuperCOSMOS data to predict a CCD V_J magnitude from a given $(B_{plt} - K_s)$ for red objects similar to those given in this paper, $(V_J - K_s) = 3.5$–9.27 or $(B_{plt} - K_s) \approx 3.7$–$10.7$, assuming a 2MASS K_s magnitude is known.

3.3. JHK_s Photometry from 2MASS

Infrared photometry in the JHK_s (hereafter simply JHK) system has been extracted from 2MASS (Skrutskie et al. 2006) and is rounded to the nearest hundredth magnitude in Table 1. All magnitudes have been checked by eye. As described in Section 4, the same 2MASS photometry has been used for both the *pltdists* and the new *ccddists* presented here. Errors are typically less than 50 mmag. Exceptions are indicated in Table 1 as superscripts to the magnitudes.

3.4. Trigonometric Parallaxes

A total of 442 southern M dwarf systems have *trigdists* placing them within 25 pc; their weighted mean parallaxes and resulting distances are listed in Tables 1 and 2. These systems have been extracted from the new RECONS 25 pc Database that contains all stellar systems with published trigonometric parallaxes of at least 40 mas and with errors less than 10 mas. The RECONS group has published the only parallax for 147 (25%) of the 581 systems with parallaxes reported in this paper. Included in that 147 are 24 systems in the lower portions of Tables 1 and 2 that have parallaxes <40 mas measured by RECONS—these were anticipated to be closer than 25 pc because of their *pltdists* and/or *ccddists*, but are now known to lie beyond 25 pc.

For all systems without parallaxes, a search of YPC and HIP was carried out in the event that a parallax <40 mas already existed. A 30′ search radius for YPC and a 5′ search radius for HIP were used in sweeps for objects to compensate for high proper motions as well as poor coordinates, the latter being particularly important for the YPC. Possible matches were then confirmed or refuted by comparing identifiers, proper motions, and V magnitudes. Seven percent (114 systems) of the entire sample in this paper were discovered to have parallaxes <40 mas in YPC and/or HIP. No other systematic literature search for stars with published parallaxes beyond 25 pc has yet been done beyond those using YPC and HIP.

4. DISTANCES

4.1. Photographic Plate Distance Estimates

The *pltdist* estimates in Table 2 are calculated by combining SuperCOSMOS *BRI* photometry with 2MASS infrared photometry via a suite of 15 color–M_K relations using *BRIJHK*, as described in Hambly et al. (2004). The four relations M_K versus $B - R$, $J - H$, $J - K$, and $H - K$ have limited spans in color through the M dwarf sequence and are thus omitted. The *pltdist* estimate is considered reliable if the remaining 11 relations are applicable, i.e., if a star's color falls within the range covered by the calibrations for single, main sequence stars. However, if a target star is blended with another source on one plate, up to five relations may drop out of the suite, yielding a less reliable *pltdist* based on 6–10 relations. We consider six relations to be the minimum number acceptable for a *pltdist* because at least two of the three *BRI* magnitudes, combined with three 2MASS measurements, provide optical/infrared colors consistent with those of normal main sequence stars. A few stars in Table 2 have *pltdists* with fewer than six relations because plate magnitudes were extracted and distances estimated after it was known that *VRI* photometry and/or trigonometric parallaxes were available. Thus the new extractions of SuperCOSMOS data simply augment the sample and provide as many distances as possible for comparisons.

As described in Hambly et al. (2004), to estimate the reliability of the *pltdists* generated from the suite of relations, single, main sequence, M dwarfs with known *trgdists* were run back through the relations to derive representative errors. The mean offsets between the *pltdists* and *trigdists* were found to be 26%. In Table 2 we list the total errors that include this systematic value combined in quadrature with the standard deviation of the up to 11 individual distances computed for a given star.

4.2. CCD Distance Estimates

The *ccddists* in Table 2 are determined using a method similar to that used for the *pltdists* and are described in Henry et al. (2004). The difference is that we use more accurate CCD *VRI* magnitudes obtained at CTIO instead of plate magnitudes from SuperCOSMOS to determine the suite of color–M_K relations. Again, the maximum number of possible relations from the combination of *VRIJHK* magnitudes is 15, but in this

case 12 relations yield useful results, as the color spreads in M_K versus $J-H$, $J-K$, and $H-K$ are limited and these relations are omitted from the suite. For stars with *VRI* from the literature rather than from our observing program, the *ccddists* were calculated using the same relation suite. All photometry is on the Johnson–Kron–Cousins system, and therefore the resulting *ccddists* are all generated in a uniform fashion.

Similar to the *pltdist*, stars with all 12 relations have *ccddists* we deem reliable (assuming the stars are single and on the main sequence), and those with 7–11 relations we deem suspect because at least one magnitude and up to five relations have dropped out of the suite. Again, some stars in Table 2 have *ccddists* with fewer than six relations because *VRI* photometry was gathered and distances estimated after it was known that trigonometric parallaxes were available. Thus the new extractions of *VRI* data simply augment the sample and provide as many distances as possible for comparisons. As described in Henry et al. (2004), to estimate the reliability of the *ccddists* generated from the suite of relations, single, main sequence M dwarfs with known *trgdists* were run back through the relations to derive representative errors. The mean offsets between the *ccddists* and *trigdists* were found to be 15%. In Table 2 we list the total errors that include this systematic value combined in quadrature with the standard deviation of the up to 12 individual distances computed for a given star. Those objects with equal magnitude companions included in unresolved photometry will have distance estimates placing them too close by a factor of 1.4. Light from fainter companions will decrease this offset, whereas light from additional unresolved companions will increase this offset.

Table 2 provides the derived data, split into the 25 pc sample (top) and systems with best quality distances beyond 25 pc (bottom). Data listed include the name of the M dwarf primary, coordinates, information on the *pltdists* (the distance, the total error, number of relations), *ccddists* (the distance, the total error, number of relations), and *trgdists* (the distance from the weighted mean of published parallaxes, the weighted mean error, and the number of parallaxes used to generate the weighted mean). These empirical values are then followed by the most reliable distance and its type. Distances based upon blended photometry are given in square brackets. Distances for subdwarfs (both confirmed and candidates) are given in curly brackets and are typically closer than estimated.

4.3. Distance Comparisons

Figure 3 shows a comparison of the *pltdists* and *ccddists* for the 739 stars that have both *BRI* and *VRI* photometry placing them within 25 pc. Only those objects thought to be single have been plotted. Error bars on individual points are omitted for clarity, but can be found for individual systems in Table 2. Total errors are typically 32% in *pltdist* and 16% in *ccddist*, and include the computed systematic errors inherent to the two techniques (26% and 15% for *pltdists* and *ccddists*, respectively), and the standard deviations of the individual estimates for each star. Because estimates from individual relations in the suites are usually quite consistent, the total errors are dominated by the adopted values for systematic errors. The dominant cause of the distance discrepancies is poor plate photometry compared to CCD photometry.

Figures 4 (343 systems) and 5 (337 systems) compare the *pltdists* and *ccddists*, respectively, to the available *trgdists* placing systems within 25 pc, again using only single objects. The average offsets are 24% for the *pltdists* and 17% for the *ccddists*, consistent with the 26% and 15% reported in Hambly et al. (2004) and Henry et al. (2004). The inherent spreads around the one-to-one lines in each plot have three causes: (1) errors in the photometry and parallaxes used to derive the relations and for the stars targeted here, (2) unresolved systems, and (3) cosmic scatter due to differences in stellar ages, compositions, and perhaps magnetic properties among the stars that are not taken into account by the color–magnitude relations. *BRI* photometry errors dominate the *pltdist* versus *trgdist* offsets, while cosmic scatter dominates the *ccddist* versus *trgdist* offsets because the *VRI* photometry and parallax errors are each only a few percent. The reduced scatter in Figure 5 again illustrates the value of obtaining accurate photometry, as the scatter has been reduced by roughly a factor of two. While it appears that the distances are more often underestimated than overestimated, this is a result of the presence of unresolved multiples and young objects in the sample.

5. RESULTS

5.1. M Dwarfs, M Subdwarfs, and M Giants

Before outlining the population results of this study, we must first verify that stars included in the final sample are, indeed, M dwarfs based on the photometry and parallaxes now available. Although our sample has been selected to include only stars with proper motions in excess of $\mu = 0\farcs18\,\mathrm{yr}^{-1}$, a few giants might be included that have extraordinary space velocities, or more likely, have erroneous proper motions. For stars without parallaxes, we use several color–color diagrams to separate dwarfs from interloping giants—an example is shown in Figure 6, which plots $(J-H)$ versus $(R-K)$. There are some objects in this sample that have a published trigonometric parallax, but for which reliable CCD *VRI* photometry does not yet exist. Those objects have been included on this plot using the plate R magnitude, rather than on the absolute-color diagram in Figure 7.

A small supplementary set of giants not in the M dwarf sample discussed here is included for comparison. These giants have been observed at the 0.9 m using the same instrument configuration as for the dwarfs. Only those objects with 2MASS magnitude quality codes of *AAA* are used in Figure 6. While there appears to be some blending of giants and dwarfs in the early M section of the plot ($(R-K) \sim 2.5$–3.5 and $(J-H) \sim 0.7$–0.8), it is unlikely that any of the presumed dwarfs with only a photometric distance estimate in that region will be giants, given the proper motion limit of this sample. It is notable that the giants separate very cleanly from the dwarfs redward of $(R-K) \sim 4$. The *VRIJHK* photometry for these objects is listed in Table 3.

Four stars in this diagram are worthy of note. We have been following the initially very interesting target CD-32 16735 on our parallax program and have measured for it a preliminary parallax of -4.69 ± 3.88 mas, essentially zero within the errors. Thus, this object is most certainly a giant. Both L173-003 and GJ0552.1 are likely unresolved binaries with odd colors from an inspection of their SuperCOSMOS images (as equal luminosity binaries will appear normal on a color–color plot). A comparison of the two available distances for L173–003 also indicates that it is an unresolved binary, as its *pltdist* (23.4 pc) is an underestimate of the true *trgdist* (47.9 pc). GJ0552.1 also

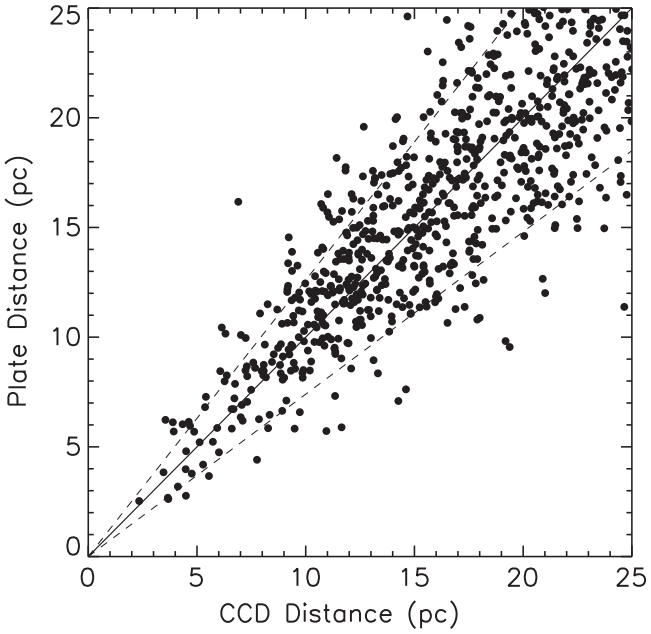

Figure 3. Distance comparisons of estimates using photographic plate photometry (*pltdist*) vs. CCD photometry (*ccddist*) for the systems closer than 25 pc that have both *BRI* and *VRI* photometry. Known unresolved multiples with blended photometry were not included. The diagonal line represents 1 : 1 correspondence in distances, while the dashed lines indicate the 26% errors associated with the plate distance estimates.

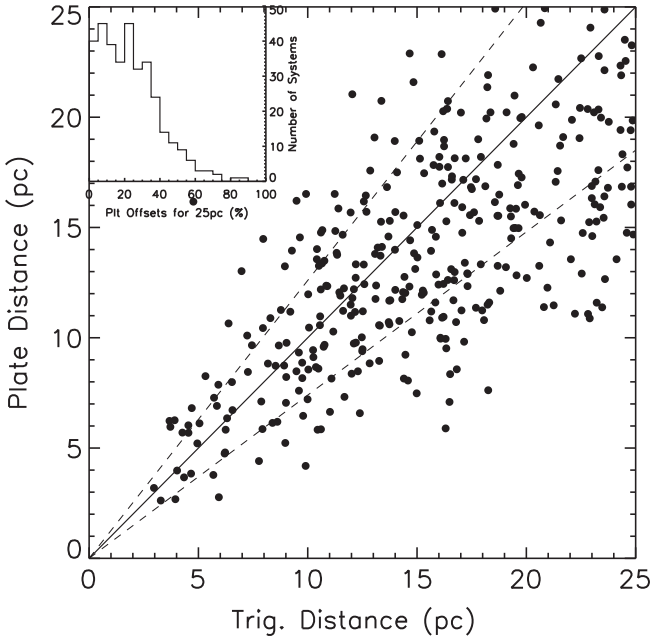

Figure 4. Distance comparisons of estimates from photographic plate photometry (*pltdist*) vs. distances measured using trigonometric parallaxes (*trgdist*) for the systems closer than 25 pc. Known unresolved multiples with blended photometry were not included. The diagonal line represents 1 : 1 correspondence in distances, while the dashed lines indicate the 26% errors associated with the plate distance estimates. The inset histogram indicates the distribution of the distance offsets between the *pltdist* and *trgdist*. For this sample, the absolute mean offset is 24%, consistent with the 26% systematic error determined in Hambly et al. (2004).

has two distances available for comparison; however they are both photometric estimates that agree within the errors: *pltdist* = 13.2 ± 5.3 versus *ccddist* = 16.3 ± 3.9. HD320012 has only a *pltdist*, but has large *H* and *K* magnitude errors.

For the roughly one-third of systems with parallaxes, confirming that they are red dwarfs is straightforward using an empirical HR diagram. An example, using M_V versus $(V - K)$, is shown in Figure 7. The M dwarf sequence is well-defined, and there is a noticeable population of cool subdwarfs below the main sequence having $(V - K) = 3.5$–4.5. As is evident from this diagram, none of the stars with trigonometric parallaxes presented in this paper fall in the region where known giants are found, so we are confident that at least among the stars with parallaxes, there are no giants.

In Figure 8 we show a reduced proper motion diagram (Boyd et al. 2011b) to confirm the subdwarfs identified in Figure 7 and to find additional subdwarf candidates in the sample that do not have parallaxes. Note that because subdwarfs are found below the main sequence (contrary to the positions of young and multiple objects above the main sequence), their distances will be *overestimated* rather than underestimated. Distances for these objects have been enclosed in curly brackets in Table 2 to highlight this effect. In total, we have identified 24 red subdwarf candidate systems, listed in Table 4. Of these 24 candidates, 21 have parallaxes, three do not, and 18 are confirmed subdwarfs (LHS2852 is buried in the mass of clustered points). While LHS3528, LHS0284, and LHS0323 both appear in (or on the border of) the subdwarf region of Figure 8, they have been shown spectroscopically to be dwarfs (Hawley et al. 1996; Jao et al. 2011). LHS0110 and SSS1444-2019 have both been identified as candidates by others (e.g., Jao et al. 2011 and Schilbach et al. 2009, respectively).

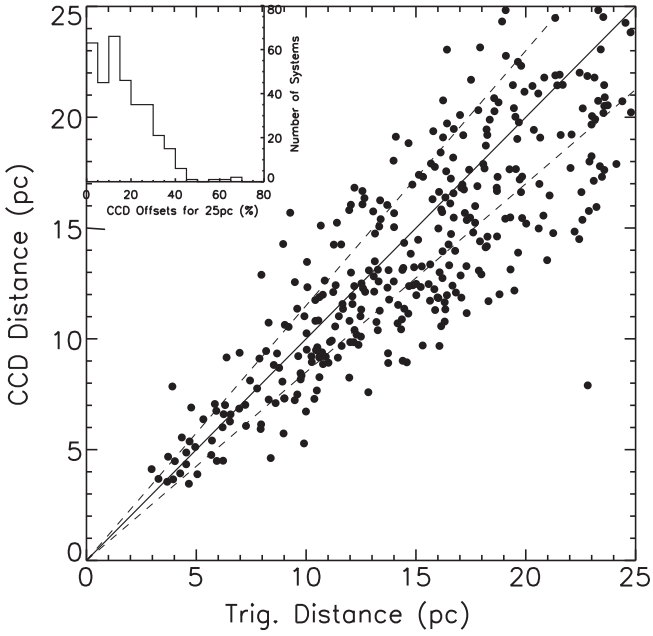

Figure 5. Distance comparisons of estimates from CCD photometry (*ccddist*) vs. distances measured using trigonometric parallaxes (*trgdist*) for the systems closer than 25 pc. Known unresolved multiples with blended photometry were not included. The diagonal line represents 1:1 correspondence in distances, while the dashed lines indicate the 15% errors associated with the CCD distance estimates. Note the reduced scatter compared to the similar *pltdist* plot shown in Figure 4, indicating the improvement in the photometry. The inset histogram indicates the distribution of the distance offsets between the *pltdist* and *trgdist*. For this sample, the absolute mean offset is 17%, consistent with the 15% systematic error determined by Henry et al. (2004).

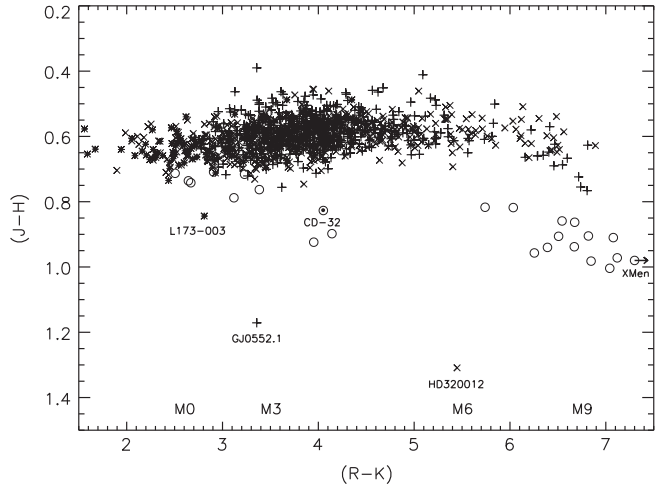

Figure 6. Color–color diagram showing $(J-H)$ vs. $(R-K)$ for all presumed single M dwarfs in the sample. Known unresolved multiples with blended photometry were not included. Colors that use plate R magnitudes are shown as x's, while those that use CCD R magnitudes are plotted as pluses. Plate R photometry is used to calculate colors for the objects for which a published parallax, but no CCD R photometry exists and are noted as asterisks with a solid center. For comparison, a few known giants are denoted by open circles. The object CD-32 16735 is plotted as a solid dot surrounded by an open circle, as it is surely a giant, given its preliminary parallax. The giant X Men is too red for the $(R-K)$ color cut-off of this plot, but has been indicated with an arrow. Corresponding spectral type estimates are given along the bottom.

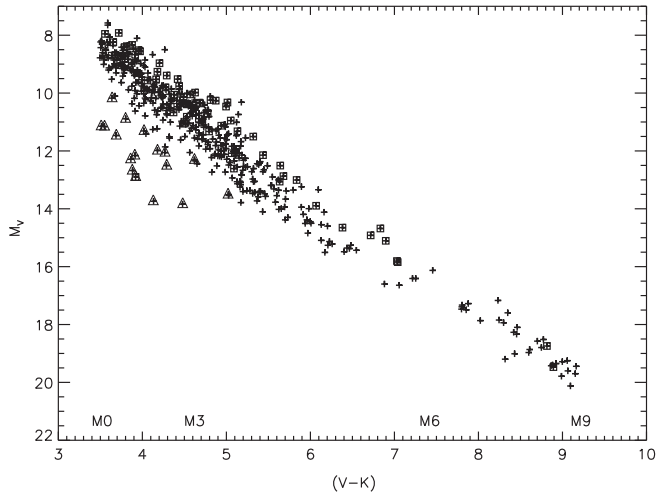

Figure 7. Observational HR diagram for all M dwarf systems in the sample that have trigonometric parallaxes and V magnitudes, using M_V and $(V-K)$ as proxies for luminosity and temperature, respectively. Known multiples with blended photometry are enclosed in open squares. A set of a few dozen subdwarfs is evident below the main sequence. Spectroscopically confirmed subdwarfs have been enclosed in triangles, with references given in Table 3. Corresponding spectral type estimates are given along the bottom.

5.2. The Red Dwarf Population

Of the 1748 systems presented here, our best distance estimates place 1404 closer than 25 pc. Table 5 lists the distance statistics for the entire sample. Those primaries with distance underestimates due to blended photometry are given in brackets next to the numbers in the multiples column. The 344 systems beyond 25 pc were typically pushed over the horizon via new *VRI* and/or new parallax measurements, or are supplementary entries to the sample with new *VRI* photometry. Even if an updated and better quality distance has moved a system beyond 25 pc, it remains in the sample for distance comparison purposes.

This sample is of sufficient size to calculate "retention rates" for stars that were first estimated to be within defined distance limits via the two photometric distance estimating techniques.

For the 1512 primaries that have *pltdists* that place them within 25 pc, 417 now have a trigonometric parallax ($\pi_{\rm trig}$) $\geqslant$ 40 mas, and 112 now have $\pi_{\rm trig} < 40$ mas, resulting in a 78.8% likelihood that an object initially estimated to be within 25 pc will be found within 25 pc. For the 904 primaries with *pltdists* $\leqslant$ 20 pc, 379 now have $\pi_{\rm trig} \geqslant 40$ mas, and 67 now have $\pi_{\rm trig} <$ 40 mas, leading to a retention rate of 85.0%. Finally, for the 443 systems with *pltdists* $\leqslant$ 15 pc, 276 now have $\pi_{\rm trig} \geqslant 40$ mas, and 18 now have $\pi_{\rm trig} < 40$ mas, giving a retention rate of 93.9%.

For the 896 primaries that have *ccddists* that place them within 25 pc, 402 now have $\pi_{\rm trig} \geqslant 40$ mas, and 32 now have $\pi_{\rm trig} < 40$ mas, giving a retention rate of 92.6%. For the 664 primaries with *ccddists* $\leqslant$ 20 pc, 359 now have $\pi_{\rm trig} \geqslant 40$ mas, and 12 now have $\pi_{\rm trig} < 40$ mas, leading to a retention rate of 96.8%. And for the 409 systems with *ccddists* $\leqslant$ 15 pc, 257 now have $\pi_{\rm trig} \geqslant 40$ mas, and 4 now have $\pi_{\rm trig} < 40$ mas, resulting in a 98.5% likelihood that an object initially estimated to be within 15 pc will be found within 25 pc.

Thus, our photometric distance estimating techniques are successful in revealing red dwarfs within 25 pc 79%–99% of the time, depending on which set of photometry is used and how restrictive the boundary is set. Even in the worst case, we are successful in nearly four out of five cases.

Figure 9 outlines the volume density of the southern M dwarfs within 25 pc, using the $(V-K)$ color versus distance in ten equal volume shells to 25 pc.[17] We expect a uniform volume density to the 25 pc horizon, and that is now the case for red dwarfs with types earlier than $\sim$ M4. Although recent work by RECONS (Dieterich et al. 2014) has bolstered the number of the closest and reddest objects on this plot, the sample shows a classic observational bias for redder, i.e., intrinsically fainter stars that are underrepresented at larger distances. There are several reasons for the non-uniform distribution, including the following. (1) The reddest dwarfs with types later than M6 have simply been missed in various search efforts, including our SCR trawls, due to their intrinsic faintness. (2) Some of the currently known 25 pc members are hidden multiples—resolution of these multiples would move the points to larger distances if they have been placed in Figure 9 using *pltdist* or *ccddist*. (3) Some systems are likely among the ~80 southern red dwarfs within 25 pc predicted to have $\mu < 0\farcs18\ {\rm yr}^{-1}$ by Riedel (2012). These have been excluded due to our proper motion cut-off. In fact, we currently have ~40 stars on our parallax program with $\mu < 0\farcs18\ {\rm yr}^{-1}$ having preliminary parallaxes larger than 40 mas. (4) Finally, some red dwarfs are lurking in the Galactic plane, which has traditionally been avoided due to crowded fields, although this deficit is not likely to be significantly distance-dependent.

We can assess the incompleteness of the current sample by assuming that the 19 southern systems with M dwarf primaries found within 5 pc (Henry 2014, pp. 286–290) represent a complete sample and that the stellar density is constant to 25 pc. If so, we expect 2375 such systems within 25 pc in the southern sky. The histogram in Figure 10 plots the cumulative

[17] For those ~500 targets that lack a V_J magnitude, one has been estimated using the polynomial given in Section 3.2.

Table 3
Comparison Photometry for Giants

Name	R.A.	Decl.	V_J (mag)	R_{KC} (mag)	I_{KC} (mag)	# Nts	J (mag)	H (mag)	K_s (mag)
TT SCL	00 16 54.6	−30 13 52	11.81	10.89	10.18	2	8.92	8.21	7.98
AF ERI	04 20 19.5	−10 24 26	13.18	10.99	8.75	2	5.80	4.94	4.45
HD270965	05 00 40.4	−71 57 53	11.38	10.62	9.94	2	8.91	8.17	7.98
DEN0515-2200	05 15 36.6	−22 00 10	13.37	12.27	10.81	2	9.32	8.42	8.13
HD269328	05 17 07.5	−70 56 38	10.41	9.70	9.04	1	8.05	7.33	7.20
SCR0629-2101	06 29 20.2	−21 01 30	15.37	12.98	10.84	1	7.82	6.91	6.47
SCR0656-2918	06 56 15.9	−29 18 03	13.89	11.72	9.45	1	6.37	5.51	5.05
SCR0703-3507	07 03 49.6	−35 07 44	15.34	12.80	10.61	1	7.35	6.37	5.95
SCR0705-3534	07 05 47.4	−35 34 26	13.95	11.70	9.39	1	6.03	5.12	4.62
SCR0833-6107	08 33 27.7	−61 07 58	13.02	11.90	10.72	1	9.63	8.87	8.52
SCR1048-7739	10 48 26.7	−77 39 19	11.47	10.53	9.64	1	8.26	7.54	7.30
SCR1317-4643	13 17 56.5	−46 43 54	13.96	12.12	10.02	1	7.57	6.75	6.38
SCR1358-4910	13 58 43.6	−49 10 52	16.14	13.91	11.62	1	8.61	7.67	7.24
SCR1440-7837	14 40 37.4	−78 37 11	10.75	9.88	9.01	1	7.71	6.92	6.76
SCR1534-7237	15 34 02.5	−72 37 11	16.03	13.94	11.71	1	8.90	7.96	7.55
SCR1544-1805	15 44 45.0	−18 05 07	13.54	11.36	9.09	1	5.96	5.05	4.54
HIP082725	16 54 32.5	−62 24 14	11.55	10.82	10.12	1	9.06	8.32	8.15
SCR2000-0837	20 00 58.3	−08 37 28	14.49	12.08	9.73	1	6.46	5.46	5.04
V506AQL	20 02 50.8	−04 32 56	13.18	10.99	8.74	1	6.14	5.18	4.74
SCR2038-0409	20 38 45.5	−04 09 27	16.44	14.01	11.65	2	8.27	7.30	6.89
2MA2108-2120	21 08 33.1	−21 20 52	14.15	12.12	9.90	2	7.31	6.49	6.09
CD-32 16735	21 47 02.7	−32 24 40	9.22	8.11	6.70	3	5.24	4.41	4.06
LEHPM2-0438	23 50 08.3	−86 51 02	11.63	10.49	9.17	2	7.69	6.77	6.54

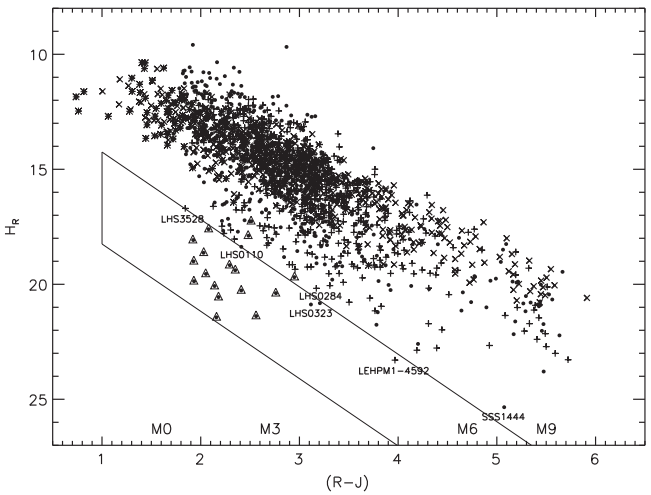

Figure 8. A reduced proper motion diagram is shown, which is used to separate the dwarfs from the subdwarfs in the entire sample, based on the proper motion of the objects. The region of interest is outlined, as in Boyd et al. (2011b). The y-axis is $H_R = R + 5 + 5\log(\mu)$ and the x-axis is the $(R - J)$ color. Primaries with *trgdists* are plotted as solid dots, those with *ccddists* are pluses, and those with *pltdists* are x's. Objects that have a published parallax, but no CCD photometry have been indicated as asterisks with a solid center. Three additional objects, among those identified as subdwarf candidates in Table 4, are shown inside the outlined subdwarf region: LHS0284, LHS0323, and LEHPM1-4592, although both LHS0284 and LHS0323 have been shown to be dwarfs (Jao et al. 2011). Spectroscopically confirmed subdwarfs have been enclosed in triangles, three of which fall outside the indicated subdwarf region and are labeled. Corresponding spectral type estimates are given along the bottom.

number of expected systems at distances to 25 pc as a solid line, with the dotted lines representing the Poisson errors. Here we have propagated the 23% error on the 19 systems within 5 pc to the aggregate number of systems within 25 pc, corresponding to an error of 546 systems in 2375. The histogram of systems outlined for the trigonometric sample is the starting point for systems we consider reliably within 25 pc. The histograms for the CCD and plate additions include only those systems with best distances that are "clean", i.e., those that are for single stars based on current information, and that are not subdwarfs. These histograms are presumably overestimates, as a fraction of the included systems are as yet undiscovered close multiples with blended photometry whose plate and CCD distances are underestimates. We do not expect these overestimates to be extreme, in part because some of the known close multiple systems purposely removed to clean the sample will remain within 25 pc. With these *caveats* in mind, we make the following assessments of our current knowledge: *We predict that there are 1829–2921 stellar systems with red dwarf primaries within 25 pc in the southern sky, we have identified roughly 1400 of these systems, based on our retention rates, only ∼90% of those with distance estimates or 1302 of these will remain within 25 pc, and there are ∼530–1620 systems missing from the current sample.*

Using the mass–M_K relation given in Henry & McCarthy (1993), masses have been estimated for each M dwarf primary in the sample that is currently believed to be a single, main sequence star. The resulting mass function, the number of stars within each mass bin, for southern primaries within 25 pc is illustrated in Figure 11. The mass function may turn over at some point, but the turnover at $\sim 0.15\,M_\odot$ indicated in this histogram is likely not the final answer. Early work by Henry & McCarthy (1990) pointed to $\sim 0.1\,M_\odot$ as the end of the main sequence and where the mass function will turn over. More recent work by Chabrier (2003) and Dieterich et al. (2012) reinforces this result. As is evident in Figure 9, few of the intrinsically faintest M dwarfs have yet to be identified beyond ∼20 pc, corresponding to roughly half of the sample volume, and these are the stars that will fill the lowest mass bins in Figure 11. Perhaps even more important, the true mass function

Table 4
Subdwarf Candidates

Name	R.A.	Decl.	μ ($''$ yr^{-1})	P.A. (deg)	d_{best} (pc)	Type	V_{tan} (km s^{-1})	Spec Typ	Ref
LHS0109	00 17 40.0	−10 46 17	1.051	180.0	35.21	trg	175	M1.0VI	4
LHS0110	00 19 37.0	−28 09 46	1.388	192.2	30.45	trg	195	M4.0JVI:	5
GJ1062	03 38 15.7	−11 29 14	2.958	152.0	16.03	trg	230	M2.5VI	1
LHS0186	04 03 38.4	−05 08 05	1.153	168.0	51.55	trg	282	M2.0VI	4
WT0135	04 11 27.1	−44 18 10	0.692	067.1	25.61	trg	84	M3.0VI	5
LHS0189	04 25 38.4	−06 52 37	1.237	145.1	18.44	trg	108	M3.0VIJ	4
GJ0191	05 11 40.6	−45 01 06	8.728	131.4	3.91	trg	162	M1.0VI	1
LHS0272	09 43 46.2	−17 47 06	1.439	279.2	13.52	trg	92	M3.0VI	1
LHS0284	10 36 03.1	−14 42 29	1.165	300.5	47.30	trg	261	M4.0 V	5
LHS0299	11 11 22.7	−06 31 56	1.073	206.9	83.33	trg	424	M0.5VI	4
LHS0323	12 17 30.2	−29 02 21	1.147	308.1	42.94	trg	225	M4.0 V	5
LHS0326	12 24 26.8	−04 43 37	1.301	241.8	49.04	trg	303	M3.0VI	4
LHS2852	14 02 46.7	−24 31 50	0.506	315.6	21.79	ccd	52	M2.0VI	1
LHS0375	14 31 38.3	−25 25 33	1.386	268.6	23.98	trg	158	M4.0VI	1
SSS1444–2019	14 44 20.3	−20 19 26	3.507	236.0	16.23	trg	270	M9.0VI:	7
LHS0381	14 50 28.9	−08 38 37	1.560	188.4	36.50	trg	270	M3.5VI	8
LHS0382	14 50 41.2	−16 56 31	1.379	243.6	48.33	trg	327	M3.5VI	3
LHS0385	14 55 35.8	−15 33 44	1.736	209.6	49.02	trg	403	M1.0VI	4
SCR1916–3638	19 16 46.6	−36 38 06	1.328	184.0	67.66	trg	426	M3.0VI	4
LHS3480	19 44 22.0	−22 30 54	0.547	139.5	56.50	trg	147	M4.0VI	1
LHS3528	20 10 55.5	−25 35 09	0.848	166.6	58.40	ccd	235	M4.5 V	2
LHS3620	21 04 25.4	−27 52 47	0.985	184.4	77.64	trg	363	M2.0VI	5
LHS0515	21 55 48.0	−11 21 43	1.093	120.3	51.28	trg	265	M3.5VI	6
LEHPM1–4592	22 21 11.4	−19 58 15	1.066	125.1	88.99	ccd	450		

References. (1) Gizis (1997), (2) Hawley et al. (1996), (3) Jao et al. (2005), (4) Jao et al. (2008), (5) Jao et al. (2011), (6) Reid & Gizis (2005), (7) Schilbach et al. (2009), (8) van Altena et al. (1995).

Table 5
Distance Statistics for Southern Red Dwarf Systems

Distance	# Systems	# Multiples	# Subdwarfs
$d \leqslant 10.0$ pc	104	24 [22]	1
$10.0 < d \leqslant 25.0$ pc	1300	140 [96]	8
$25.0 < d \leqslant 100.0$ pc	343	33 [15]	18
TOTAL	1747[a]	197	27[b]

Note. Numbers in brackets indicate systems with unresolved photometry, some of which were used to calculate distance estimates that are likely underestimates.
[a] CD-32 16735 is beyond 100 pc and is not included in this total.
[b] Two of the subdwarf systems are binaries, and thus are also included in the "Multiples" counts column.

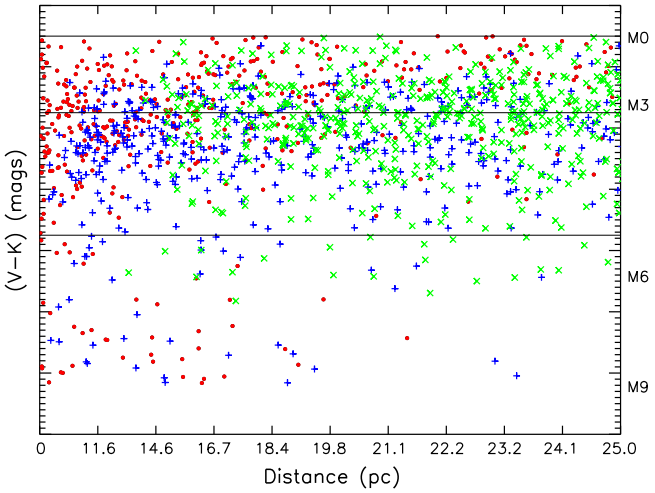

Figure 9. Density of M dwarf systems in the southern sky plotted using $(V - K)$ vs. distance in 10 equal-volume shells to 25 pc. Solid points indicate systems with *trgdists*, pluses indicate those with *ccddists*, and x's indicate those with *pltdists*. Corresponding spectral type estimates are given along the right. For those 507 objects without a CCD V magnitude, one has been estimated using the Equation in Section 3.2. The horizontal lines highlight masses of 0.60, 0.30, and 0.10 $M_{\odot}$ from top to bottom.

for low mass stars will include M dwarfs as companions, and both known and as yet unknown fainter companions to M dwarf primaries in the sample will shift points to lower masses. This makes a profound statement that the smallest stars are the most likely product of the stellar/substellar formation process.

6. FUTURE

Of the 1404 southern M dwarf systems presented here as within 25 pc, 954 do not have published parallaxes. More than 250 objects with only distances estimates are on our astrometry program at the 0.9 m. If these systems lacking a parallax turn out to be within 25 pc, the RECONS effort in the southern sky will have increased the number of stellar systems identified within this distance by 52%.

Of course, *Gaia* should make great contributions to the census of nearby red dwarfs. However, assuming its $V \approx 20$

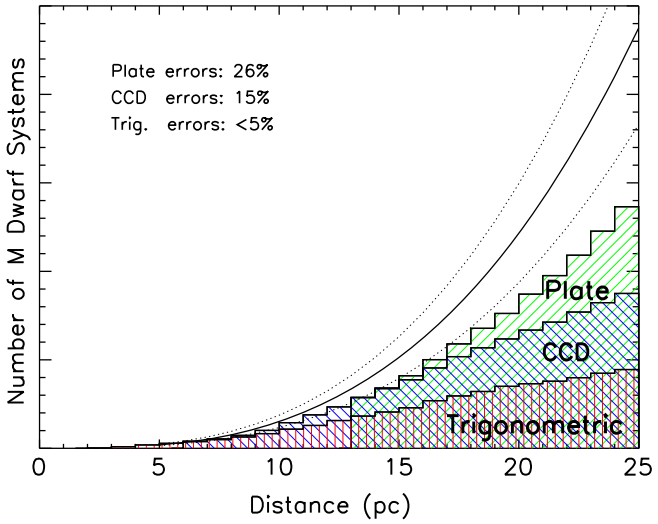

Figure 10. Cumulative numbers of southern single M dwarf systems known via the three distance techniques described in this paper are shown using histograms. Those objects with *trgdists* are indicated with vertical hatching, those with *ccddists* have −45° hatching and those with *pltdists* have +45° hatching. The solid black curve indicates the expected number within that distance horizon based on the 19 southern M dwarf systems known to lie within 5 pc with accurate trigonometric parallaxes and assuming a uniform density to 25 pc. The dotted lines indicate the extrapolated 23% Poisson errors based on those 19 systems.

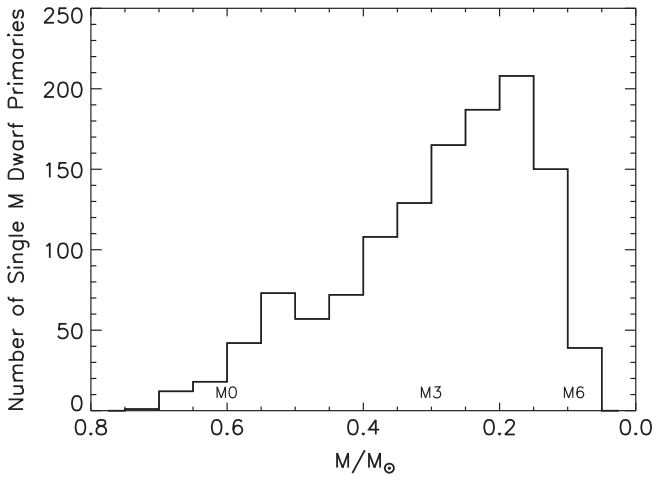

Figure 11. Mass function for southern single M dwarf primaries known within 25 pc is shown. Not included are the 100 primaries with blended photometry due to the presence of a close companion. Those objects with mass estimates greater than 0.6 $M_{\odot}$ are possibly unknown unresolved close multiples. The apparent turnover at ∼0.15 $M_{\odot}$ is likely not the final answer.

limit (Sozzetti et al. 2014) is achieved, it will only reach the intrinsically faintest M dwarfs to about 10 pc. Thus, it appears that careful, pointed observations to reveal the M dwarfs within 25 pc remain warranted and will be crucial in determining the true mass function for the smallest stars.

This research was made possible by NSF grants AST-0908402 and AST-1109445. The support of additional RECONS team members was vital for this research. We also thank the members of the SMARTS Consortium, who enable the operations of the small telescopes at CTIO, as well as the observer support at CTIO, specifically Edgardo Cosgrove, Arturo Gomez, Alberto Miranda, Joselino Vasquez, Mauricio Rojas, and Hernan Tirado. We would like to thank Rick Mascall for bringing to our attention the object OUT1720-1725. The authors are grateful to referee Bill van Altena for suggesting changes that improved the paper.

This research has made use of data obtained from the SuperCOSMOS Science Archive, prepared and hosted by the Wide Field Astronomy Unit, Institute for Astronomy, University of Edinburgh, which is funded by the UK Science and Technology Facilities Council. Data products from the Two Micron All Sky Survey, which is a joint project of the University of Massachusetts and the Infrared Processing and Analysis Center/California Institute of Technology, funded by the National Aeronautics and Space Administration and the National Science Foundation have also been used, as have the SIMBAD database and the Aladin and VizieR interfaces, operated at CDS, Strasbourg, France.

REFERENCES

Andrei, A. H., et al. 2011, AJ, 141, 54
Anglada-Escudé, G., Boss, A. P., Weinberger, A. J., et al. 2012, ApJ, 746, 37
Benedict, G. F., et al. 2002, ApJ, 581, L115
Bessel, M. S. 1990, A&AS, 83, 357
Bessell, M. S. 1991, AJ, 101, 662
Bessell, M. S., & Weis, E. W. 1987, PSAP, 99, 642
Biller, B. A., & Close, L. M. 2007, ApJ, 669, L41
Boyd, M. R., Henry, T. J., Jao, W.-C., Subasavage, J. P., & Hambly, N. C. 2011a, AJ, 142, 92
Boyd, M. R., Winters, J. G., Henry, T. J., et al. 2011b, AJ, 142, 10
Chabrier, G. 2003, PASP, 115, 763
Costa, E., & Méndez, R. A. 2003, A&A, 402, 541
Costa, E., Méndez, R. A., Jao, W.-C., et al. 2005, AJ, 130, 337
Costa, E., Méndez, R. A., Jao, W.-C., et al. 2006, AJ, 132, 1234
Deacon, N. R., & Hambly, N. C. 2001, A&A, 380, 148
Deacon, N. R., & Hambly, N. C. 2007, A&A, 468, 163
Deacon, N. R., Hambly, N. C., & Cooke, J. A. 2005a, A&A, 435, 363
Deacon, N. R., Hambly, N. C., Henry, T. J., et al. 2005b, AJ, 129, 409
Deacon, N. R., Hambly, N. C., King, R. R., & McCaughrean, M. J. 2009a, MNRAS, 394, 857
Deacon, N. R., et al. 2009b, MNRAS, 397, 1685
Dieterich, S. B., Henry, T. J., Golimowski, D. A., Krist, J. E., & Tanner, A. M. 2012, AJ, 144, 64
Dieterich, S. B., Henry, T. J., Jao, W.-C., et al. 2014, AJ, 147, 94
Dupuy, T. J., & Liu, M. C. 2012, ApJS, 201, 19
Fabricius, C., & Makarov, V. V. 2000, A&AS, 144, 45
Faherty, J. K., et al. 2012, ApJ, 752, 56
Finch, C. T., Henry, T. J., Subasavage, J. P., Jao, W.-C., & Hambly, N. C. 2007, AJ, 133, 2898
Finch, C. T., Zacharias, N., Boyd, M. R., Henry, T. J., & Hambly, N. C. 2012, ApJ, 745, 118
Finch, C. T., Zacharias, N., & Henry, T. J. 2010, AJ, 140, 844
Fischer, D. A., & Marcy, G. W. 1992, ApJ, 396, 178
Gatewood, G., Coban, L., & Han, I. 2003, AJ, 125, 1530
Giclas, H. L., Burnham, R., & Thomas, N. G. 1971, in Lowell Proper Motion Survey Northern Hemisphere. The G Numbered Stars. 8991 Stars Fainter than Magnitude 8 with Motions gt 0.″26/year (Flagstaff, AZ: Lowell Observatory)
Giclas, H. L., Burnham, R., Jr, & Thomas, N. G. 1978, LowOB, 8, 89
Gizis, J. E. 1997, AJ, 113, 806
Gizis, J. E., Troup, N. W., & Burgasser, A. J. 2011, ApJ, 736, L34
Graham, J. A. 1982, PASP, 94, 244
Hambly, N. C., Henry, T. J., Subasavage, J. P., Brown, M. A., & Jao, W.-C. 2004, AJ, 128, 437
Hambly, N. C., Irwin, M. J., & MacGillivray, H. T. 2001, MNRAS, 326, 1295
Hawley, S. L., Gizis, J. E., & Reid, I. N. 1996, AJ, 112, 2799
Henry, T. J. 1991, PhD thesis, Univ. Arizona
Henry, T. J. 2014, in The Observer's Handbook, ed. D. M. F. Chapman (Toronto, ON: The Royal Astronomical Society of Canada)
Henry, T. J., Ianna, P. A., Kirkpatrick, J. D., & Jahreiss, H. 1997, AJ, 114, 388
Henry, T. J., Jao, W.-C., Subasavage, J. P., et al. 2006, AJ, 132, 2360

Henry, T. J., & McCarthy, D. W., Jr 1990, ApJ, 350, 334
Henry, T. J., & McCarthy, D. W., Jr 1993, AJ, 106, 773
Henry, T. J., Subasavage, J. P., Brown, M. A., et al. 2004, AJ, 128, 2460
Hershey, J. L., & Taff, L. G. 1998, AJ, 116, 1440
Høg, E., et al. 2000, A&A, 355, L27
Janson, M., et al. 2012, ApJ, 754, 44
Janson, M., Bergfors, C., Brandner, W., et al. 2014, ApJ, 789, 102
Jao, W.-C., Henry, T. J., Beaulieu, T. D., & Subasavage, J. P. 2008, AJ, 136, 840
Jao, W.-C., Henry, T. J., Subasavage, J., et al. 2014, AJ, 147, 21
Jao, W.-C., Henry, T. J., Subasavage, J. P., et al. 2005, AJ, 129, 1954
Jao, W.-C., Henry, T. J., Subasavage, J. P., et al. 2011, AJ, 141, 117
Kilkenny, D., & Cousins, A. W. J. 1995, Ap&SS, 230, 155
Kilkenny, D., Koen, C., van Wyk, F., Marang, F., & Cooper, D. 2007, MNRAS, 380, 1261
Kilkenny, D., van Wyk, F., Roberts, G., Marang, F., & Cooper, D. 1998, MNRAS, 294, 93
Koen, C., Kilkenny, D., van Wyk, F., Cooper, D., & Marang, F. 2002, MNRAS, 334, 20
Koen, C., Kilkenny, D., van Wyk, F., & Marang, F. 2010, MNRAS, 403, 1949
Landolt, A. U. 1992, AJ, 104, 372
Landolt, A. U. 2007, AJ, 133, 2502
Landolt, A. U. 2013, AJ, 146, 131
Lépine, S. 2005a, AJ, 130, 1680
Lépine, S. 2005b, AJ, 130, 1247
Lépine, S. 2008, AJ, 135, 2177
Lépine, S., & Gaidos, E. 2011, AJ, 142, 138
Lépine, S., Shara, M. M., & Rich, R. M. 2002, AJ, 124, 1190
Lépine, S., Shara, M. M., & Rich, R. M. 2003, AJ, 126, 921
Luyten, W. J. 1979a, in LHS Catalogue (Minneapolis, MN: Univ. of Minnesota)
Luyten, W. J. 1979b, in NLTT Catalogue (Minneapolis, MN: Univ. of Minnesota)
Luyten, W. J. 1980a, in NLTT Catalogue (Minneapolis, MN: Univ. of Minnesota)
Luyten, W. J. 1980b, in NLTT Catalogue (Minneapolis, MN: Univ. of Minnesota)
Mamajek, E. E., Bartlett, J. L., Seifahrt, A., et al. 2013, AJ, 146, 154
Monet, D. G., Levine, S. E., Canzian, B., et al. 2003, AJ, 125, 984
Morgan, D. H. 1995, in ASP Conf. Ser. 84, Proc. IAU Coll.: 148: The Future Utilisation of Schmidt Telescopes, ed. J. Chapman, et al. (San Francisco, CA: ASP), 137
Patterson, R. J., Ianna, P. A., & Begam, M. C. 1998, AJ, 115, 1648
Phan-Bao, N. 2011, AN, 332, 668
Pokorny, R. S., Jones, H. R. A., & Hambly, N. C. 2003, A&A, 397, 575
Pokorny, R. S., Jones, H. R. A., Hambly, N. C., & Pinfield, D. J. 2004, A&A, 421, 763
Reid, I. N., & Gizis, J. E. 2005, PASP, 117, 676
Reid, I. N., Kilkenny, D., & Cruz, K. L. 2002, AJ, 123, 2822
Reid, I. N., van Wyk, F., Marang, F., et al. 2001, MNRAS, 325, 931
Reid, I. N., Cruz, K. L., Allen, P., et al. 2003, AJ, 126, 3007
Reid, I. N., Cruz, K. L., Allen, P., et al. 2004, AJ, 128, 463
Riedel, A. R. 2012, PhD thesis, Georgia State Univ.
Riedel, A. R., Murphy, S. J., Henry, T. J., et al. 2011, AJ, 142, 104
Riedel, A. R., Subasavage, J. P., Finch, C. T., et al. 2010, AJ, 140, 897
Riedel, A. R., Finch, C. T., Henry, T. J., et al. 2014, AJ, 147, 85
Ruiz, M. T., Takamiya, M. Y., Mendez, R., Maza, J., & Wishnjewsky, M. 1993, AJ, 106, 2575
Ruiz, M. T., Wischnjewsky, M., Rojo, P. M., & Gonzalez, L. E. 2001, ApJS, 133, 119
Schilbach, E., Röser, S., & Scholz, R.-D. 2009, A&A, 493, L27
Schmidt, S. J., Cruz, K. L., Bongiorno, B. J., Liebert, J., & Reid, I. N. 2007, AJ, 133, 2258
Scholz, R.-D., Lehmann, I., Matute, I., & Zinnecker, H. 2004, A&A, 425, 519
Shkolnik, E. L., Anglada-Escudé, G., Liu, M. C., et al. 2012, ApJ, 758, 56
Skrutskie, M. F., et al. 2006, AJ, 131, 1163
Smart, R. L., Ioannidis, G., Jones, H. R. A., Bucciarelli, B., & Lattanzi, M. G. 2010, A&A, 514, A84
Smart, R. L., Lattanzi, M. G., Jahreiß, H., Bucciarelli, B., & Massone, G. 2007, A&A, 464, 787
Söderhjelm, S. 1999, A&A, 341, 121
Sozzetti, A., Giacobbe, P., Lattanzi, M. G., et al. 2014, MNRAS, 437, 497
Subasavage, J. P., Henry, T. J., Hambly, N. C., Brown, M. A., & Jao, W.-C. 2005, AJ, 129, 413
Subasavage, J. P., Henry, T. J., Hambly, N. C., et al. 2005, AJ, 130, 1658
Subasavage, J. P., Jao, W.-C., Henry, T. J., et al. 2009, AJ, 137, 4547
Tinney, C. G. 1996, MNRAS, 281, 644
Tinney, C. G., Reid, I. N., Gizis, J., & Mould, J. R. 1995, AJ, 110, 3014
van Altena, W. F., Lee, J. T., & Hoffleit, D. 1995, yCat, 1174, 0
van Leeuwen, F. (ed.) 2007, *Hipparcos* the New Reduction of the Raw Data (ASSL, Vol. 350; Berlin: Springer)
von Braun, K., et al. 2011, ApJ, 729, L26
Weis, E. W. 1984, ApJS, 55, 289
Weis, E. W. 1986, AJ, 91, 626
Weis, E. W. 1987, AJ, 93, 451
Weis, E. W. 1988, Ap&SS, 142, 223
Weis, E. W. 1991a, AJ, 102, 1795
Weis, E. W. 1991b, AJ, 101, 1882
Weis, E. W. 1993, AJ, 105, 1962
Weis, E. W. 1994, AJ, 107, 1135
Weis, E. W. 1996, AJ, 112, 2300
Weis, E. W. 1999, AJ, 117, 3021
Winters, J. G., Henry, T. J., Jao, W.-C., et al. 2011, AJ, 141, 21
Wolf, M., & Reinmuth, K. 1925, AN, 223, 231
Wroblewski, H., & Costa, E. 1999, A&AS, 139, 25
Wroblewski, H., & Costa, E. 2000, A&AS, 142, 369
Wroblewski, H., & Costa, E. 2001, A&A, 367, 725
Wroblewski, H., & Torres, C. 1989, A&AS, 78, 231
Wroblewski, H., & Torres, C. 1990, A&AS, 83, 317
Wroblewski, H., & Torres, C. 1991, A&AS, 91, 129
Wroblewski, H., & Torres, C. 1992, A&AS, 92, 449
Wroblewski, H., & Torres, C. 1994, A&AS, 105, 179
Wroblewski, H., & Torres, C. 1995, A&AS, 110, 27
Wroblewski, H., & Torres, C. 1996, A&AS, 115, 481
Wroblewski, H., & Torres, C. 1997, A&AS, 122, 447
Wroblewski, H., & Torres, C. 1998, A&AS, 128, 457